

Viscous stabilization of the invasion front in drainage displacement

Eyyvind Aker*, Knut Jørgen Måløy

Department of Physics, University of Oslo, N-0316 Oslo, Norway

Alex Hansen

Department of Physics, Norwegian University of Science and Technology, N-7491 Trondheim, Norway

(April 7, 2019)

We investigate the stabilization mechanisms due to viscous forces of the invasion front in drainage displacement in two dimensional porous media using a network simulator. We find that in horizontal displacement the capillary pressure difference between two different points along the front vary linearly as function of height separation in the direction of the displacement. We conclude that existing theory from percolation fails to describe our simulation results. We have also compared our results with some experimental data and find that the width of the front scales similar to gravitational stabilization.

47.55.Mh, 07.05.Tp

Immiscible displacement of one fluid by another fluid in porous media generates front structures and patterns ranging from compact to ramified and fractal [1,2,3,4]. When a nonwetting fluid displaces a wetting fluid (drainage) at low injection rate, the nonwetting fluid generates a pattern of fractal dimension similar to the cluster formed by invasion percolation [5,6,7,8]. The displacement is controlled solely by the capillary pressure P_c , that is the pressure difference between the two fluids across a pore meniscus. At high injection rate and when the viscosity of the nonwetting fluid is higher or equal to the viscosity of the wetting fluid, the width of the displacement front stabilizes and a more compact pattern is generated [3,9]

When the displacement is oriented out of the horizontal plane, gravity may stabilize the front width due to density differences between the fluids [10,11]. The process has been linked to invasion percolation with a stabilizing gradient [10,11,12], and the saturated front width w_s , is found to depend on the strength of the gravity like $w_s \propto B_o^{-\nu/(1+\nu)}$. Here $B_o = \Delta\rho g a^2 / \gamma$ is the bond number indicating the ratio of gravity to capillary forces and ν is the correlation length exponent from percolation theory. Moreover, $\Delta\rho$ denotes the density differences of the fluids, g is the acceleration due to gravity, a is the typical pore size, and γ denotes the fluid interface tension.

Wilkinson [10] used percolation theory to deduce a power law between w_s and the capillary number C_a , when only viscous forces stabilize the front (horizontal displacement). He found $w_s \propto C_a^{-\nu/(1+t-\beta+\nu)}$, where C_a is the ratio of viscous to capillary forces, t is the conductivity exponent, and β is the order parameter exponent. In the following $C_a \equiv Q\mu_{nw}/\Sigma\gamma$, where Q denotes the injection rate, Σ is the cross section of the inlet and μ_{nw} denotes the viscosity of the nonwetting phase. Later on, Xu *et al.* [13] used Wilkinson's arguments to show that the pressure drop across a height difference

Δh in the nonwetting phase along the front should scale as $\Delta P_{nw} \propto \Delta h^{t/\nu+d_e-1-\beta/\nu}$. Here d_e is the Euclidean dimension of the space embedded by the front. In two dimension their result yields $\Delta P_{nw} \propto \Delta h^{1.9}$. Moreover, they argued that the corresponding pressure drop in the wetting phase ΔP_w , must be linearly dependent on Δh according to the compact displaced fluid (see Fig. 1).

The purpose of the present letter is to investigate the stabilization mechanisms of the front due to viscous and capillary forces. We consider two-dimensional horizontal drainage, thus neglecting the gravity force. We present simulations where we have calculated the capillary pressure difference ΔP_c , between two different pore menisci along the front separated a height Δh in the direction of the displacement. The simulations are based on a network model that properly describe the dynamics of the fluid-fluid displacement as well as the capillary and viscous pressure buildup. Simulations show that for a wide range of injection rates and different fluid viscosities ΔP_c varies linearly with Δh (Figs. 2 and 3). Assuming a power law behavior $\Delta P_c \propto \Delta h^\kappa$ our best estimate of the exponent is $\kappa = 1.0 \pm 0.1$. This is a surprisingly simple result and not expected because the viscous force field are non homogeneous, due to the trapping of fluid behind the front and the fractal behavior of the front structure.

According to Xu *et al.* [13] $\Delta P_c = \Delta P_{nw} - \Delta P_w$ (Fig. 1). At low injection rate or when the viscosity of the nonwetting fluid is much higher than the viscosity of the wetting one, we may neglect the pressure drop in the wetting fluid giving $\Delta P_c \sim \Delta P_{nw} \propto \Delta h^{1.9}$. Hence, the argument of Xu *et al.* is in conflict with our result which we find to be similar to gravitational stabilization where $\Delta P_c = \Delta\rho g \Delta h \propto \Delta h$ [10,11]. We have also computed the saturated front width w_s , and compared our results to experiments performed by Frette *et al.* [9]. We show that since ΔP_c behaves as if gravity stabilizes the front we may substitute B_o with C_a , giving that w_s should scale with C_a like $w_s \propto C_a^{-\nu/(1+\nu)}$. Experimental work

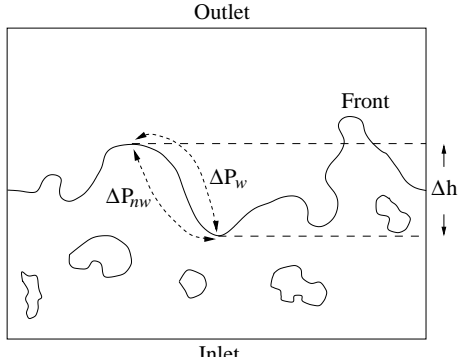


FIG. 1. A schematic picture of the front region that travels across the system from the inlet to the outlet. ΔP_{nw} and ΔP_w denote the pressure drop along the front over the distance Δh in the nonwetting and wetting fluid respectively. The capillary pressure difference between two menisci separated a height Δh is $\Delta P_c \simeq \Delta P_{nw} - \Delta P_w$.

of Frette *et al.* [9] confirm this results (Fig. 4).

The model porous medium consists of a square lattice of cylindrical tubes oriented at 45° . Four tubes meet at each node in the lattice, and the tubes represent the volume of both pores and throats. The tubes have equal length d , and their radii r is chosen at random inside an interval (see below) introducing the disorder in the system. The tube network is initially filled with a wetting fluid of viscosity μ_w and a nonwetting fluid of viscosity $\mu_{nw} \geq \mu_w$ is injected at the bottom row (inlet). The viscosity ratio M , is defined as $M \equiv \mu_{nw}/\mu_w$. The wetting fluid is displaced and flows out along the top row (outlet). There are periodic boundary condition in the horizontal direction. The fluids are assumed immiscible, hence an interface (a meniscus) is generated where the fluids meet in the tubes. The capillary pressure p_c , of the menisci is chosen to $p_c = (2\gamma/r) [1 - \cos(2\pi x/d)]$. The first term is Young-Laplace law for cylindrical tube when perfect wetting is assumed and in the second term x is the position of the meniscus in the tube, i.e. $0 \leq x \leq d$. Thus, with respect to the capillary pressure we treat the tubes as if they were hourglass shaped with effective radii following a smooth function. By letting p_c vary as above we include the effect of local readjustments of the menisci at pore level [14] which is important for the description of burst dynamics [15,16]. This detailed modeling of the capillary pressure costs computation time. However, it is necessary in order to properly simulate the capillary pressure behavior along the front.

The volume flux q_{ij} through a tube between the i th and the j th node is given by Washburn equation [17],

$$q_{ij} = -(\sigma_{ij} k_{ij}/\mu_{ij})(p_j - p_i - p_{c,ij})/d. \quad (1)$$

Here k_{ij} is the permeability of the tube ($r_{ij}^2/8$), σ_{ij} is the cross section (πr_{ij}^2) of the tube, p_i and p_j is the nodal

pressures at node i and j respectively, and $p_{c,ij}$ is the sum of the capillary pressures of the menisci inside the tube. A tube partially filled with both liquids, is allowed to contain either one or two menisci. Furthermore, μ_{ij} denotes the effective viscosity given by the sum of the volume fractions of each fluid inside the tube multiplied by their respective viscosities. At each node we have conservation of volume flux giving

$$\sum_j q_{ij} = 0, \quad (2)$$

so that Eq. (1) and Eq. (2) constitute a set of linear equations which are to be solved for the nodal pressures p_j . The set of equations is solved by using the Conjugate Gradient method [18] with the constraint that the injection rate Q is held constant. See Refs. [14] and [19] for further details of how p_j is found.

Given the solution of p_j we calculate the volume flux q_{ij} through each tube ij and define a time step Δt , such that every meniscus is allowed to travel at most a maximum step length Δx_{\max} , during that time step. The menisci are moved a distance $(q_{ij}/\sigma_{ij})\Delta t$ and menisci that are moved out of a tube are spread into neighbor tubes [14,19]. Numerical simulations show that to calculate the variations in the capillary pressure as menisci travel through tubes, we must choose $\Delta x_{\max} \leq 0.1d$.

Due to the computational effort, the lattice sizes used in the simulations are limited to 25×35 and 40×60 nodes. To study the behavior of ΔP_c on larger lattices, we have generated invasion percolation (IP) clusters with a stabilizing gradient on lattices of 200×300 nodes. The IP clusters are assumed to be statistical equal with same fractal dimension [9], to corresponding structures that would have been obtain in a complete displacement process. Thus, to save computation time, the generated IP clusters were loaded into our network model, and the displacement simulations were run a few number of time steps from this point.

The front between the invading and the defending fluid is detected by running a Hoshen-Kopelman algorithm [20] on the lattice. The front width w is defined as the standard deviation of the distances between each meniscus along the front and the average front position. ΔP_c is approximatively defined in Fig. 1. However, in the simulations ΔP_c is equal to the mean of the capillary pressure differences between all pairs of menisci separated a vertical distance Δh along the front. The capillary pressure difference between a pair of menisci is always calculated by taking the capillary pressure of the meniscus closest to the inlet minus the capillary pressure of the meniscus closest to the outlet.

The simulations on the 25×35 nodes lattice were performed with $\mu_{nw} = 10$ P, $\mu_w = 0.10$ P (i.e. $M = 100$) and $\gamma = 30$ dyn/cm at six different C_a between 1.1×10^{-2} and 3.7×10^{-4} by varying the injection rate. At each C_a we did 30 simulations with different sets of random radii in

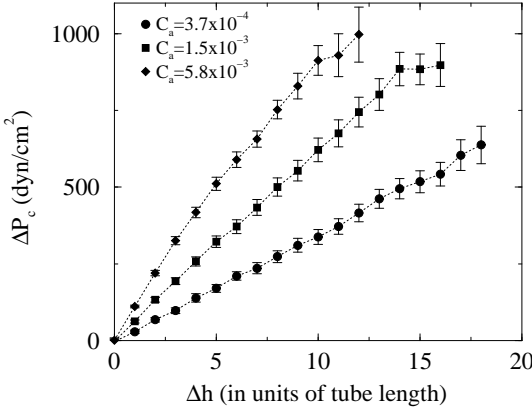


FIG. 2. ΔP_c as function of Δh for some C_a at $M = 100$. At each C_a , ΔP_c is the average of 30 different runs and the error bars denote the standard error of the mean.

the interval $0.05d \leq r_{ij} \leq d$ and tube length $d = 0.1$ cm. ΔP_c was recorded and the result for some C_a is shown in Fig. 2. We observe that ΔP_c increases roughly linearly as function of Δh . At lowest C_a the front was found to stabilize due to the finite size of the system. At higher C_a the viscous gradient stabilizes the front. The gradient causes the capillary pressure of the menisci closest to the inlet to exceed the capillary pressure of the menisci lying in the uppermost part. Thus, the menisci closest to the inlet will more easily penetrate a narrow tube compared to menisci further down the stream. This will eventually stabilize the front.

The IP clusters were generated on the bonds in a square lattice with the bonds oriented at 45° . Hence, the bonds correspond to the tubes in our network model. Each bond ij were assigned a random number f_{ij} in the interval $[0, 1]$. A stabilizing gradient $G = 0.05$, was applied giving an occupation threshold t_{ij} of every bond, $t_{ij} = f_{ij} + Gh_{ij}$ [10,11]. Here h_{ij} denotes the height of bond ij above the bottom row. The occupation of bonds started at the bottom row, and the next bond to be occupied was always the bond with the lowest threshold value from the set of empty bonds along the invasion front. When the invasion front became well developed with clusters of sizes between the bond length and the front width, the IP clusters were loaded into our network model. The radii r_{ij} of the tubes were mapped to the random numbers f_{ij} of the bonds as $r_{ij} = [0.05 + 0.95(1 - f_{ij})]d$. Thus, $0.05d \leq r_{ij} \leq d$ and as above we set the tube length $d = 0.1$ cm. We map r_{ij} to $1 - f_{ij}$ because in IP the next bond to be invaded is the one with the lowest threshold value, opposite to the network model, where the widest tube will be invaded first.

Four IP clusters were generated on different sets of f_{ij} and loaded into our network model. An injection rate Q was chosen in correspondence to G and the sim-

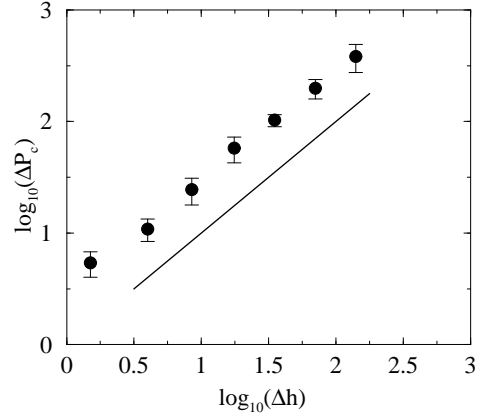


FIG. 3. $\log_{10}(\Delta P_c)$ as function of $\log_{10}(\Delta h)$ for drainage simulations initiated on IP clusters at $C_a = 1.7 \times 10^{-4}$. The result is averaged over four different runs and the error bars denote the standard error in the mean. The slope of the solid line is 1.0.

ulations were run a limited number of time steps. The number of time steps where chosen sufficiently large to let the menisci along the front adjust according to the viscous pressure set up by the injection rate. The result of the calculated ΔP_c versus Δh is shown in Fig. 3. If we assume the power law behavior $\Delta P_c \propto \Delta h^\kappa$ we find $\kappa = 1.0 \pm 0.1$. The slope of the straight line in Fig. 3 is 1.0. The result in Fig. 1 corresponds to simulations with $M = 100$, and we obtained similar result with $M = 1.0$ (viscosity matched fluids).

Frette *et al.* [9] performed two phase drainage displacement experiments in a two dimensional porous medium with viscosity matched fluids, $M = 1.0$. They reported on the stabilization of the front and measured the saturated front width w_s as function of capillary number. We have run drainage simulations with similar fluid viscosities, interface tension and pore sizes as in [9]. The lattice size was 40×60 nodes and the length of the tubes where chosen at random in the interval $0.02 \text{ cm} \leq d \leq 0.18 \text{ cm}$. The radii of the tubes were given by the aspect ratio $d/2r = 1.25$. Thus, we are effectively dealing with a distorted square lattice of tubes.

The simulations were run at different C_a by varying the injection rate, and the calculated w_s together with the experimental result in [9] is shown in Fig. 4 as function of C_a . If we assume a power law behavior like $w_s \propto C_a^{-\alpha}$ our best estimate of the exponent due to the simulations is $\alpha = 0.3 \pm 0.1$. Simulations performed in [13] resembles with our result. In [9] $\alpha = 0.6 \pm 0.2$ was found experimentally, indicated by the solid line in Fig. 4, and in two dimensions Wilkinson's argument [10] gives $\alpha = \nu/(1+t-\beta+\nu) \approx 0.38$. The Wilkinson argument lies within the uncertainties of our simulation result. However, in Fig. 4 there seems to be a crossover in the scal-

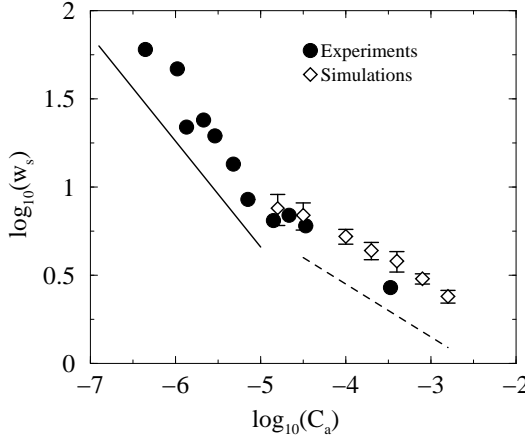


FIG. 4. $\log_{10}(w_s)$ as function of $\log_{10}(C_a)$ for experiments from [9] and simulations on a lattice of 40×60 nodes. For both experiments and simulations $M = 1.0$. The slope of the solid and dashed line is -0.6 and -0.3 respectively.

ing behavior. For $C_a \gtrsim 1.0 \times 10^{-5}$ the simulations fits $\alpha = 0.3$ which also seems to be consistent with the experiments despite the few experimental data points in this regime. For $C_a \lesssim 1.0 \times 10^{-5}$ the experiments match $\alpha = 0.6$. The crossover lead to the following considerations. The injection rate Q sets the strength of the viscous pressure gradient resulting in the capillary pressure difference ΔP_c . Thus, it is reasonable that $\Delta P_c \propto C_a \Delta h^\kappa$ where our simulations show that $\kappa = 1.0 \pm 0.1$. When gravity stabilizes the front the analog to this relation is $\Delta P_c \propto B_o \Delta h$. Hence, ΔP_c is linearly dependent on Δh for both viscous and gravitational stabilization. At sufficiently low injection rate where the displacement is close to capillary equilibrium, percolation concepts yields $\Delta P_c \propto f - f_c \propto \xi^{-1/\nu}$ [12,10,11]. Here f is the occupation probability of the bonds, f_c is the percolation threshold, and ξ is the correlation length. In the simulations the correlation length corresponds to the front width, and therefore we obtain $\xi \propto w_s \propto C_a^{-\nu/(1+\nu)}$. Inserting $\nu = 4/3$ gives $w_s \propto C_a^{-0.57}$, which is close to the experimental result of Frette *et al.* [9] when $C_a \lesssim 1.0 \times 10^{-5}$ (Fig. 4). At higher $C_a \gtrsim 1.0 \times 10^{-4}$ the displacement is no longer in capillary equilibrium and percolation concepts cannot be applied. Thus, we expect as observed in Fig. 4, another type of scaling behavior there. At lower $C_a \simeq 1.0 \times 10^{-5}$ the width of the front in our simulations becomes bounded by the lattice size and a further reduction in C_a does not give rise to wider front. Therefore with our simulations, we don't expect to observe the $w_s \propto C_a^{-0.57}$ regime. Note, however, that the power law $\Delta P_c \propto \Delta h^\kappa$, where $\kappa = 1.0$ is found to be valid for both low and high capillary numbers.

In summary we conclude that $\Delta P_c \propto \Delta h^\kappa$ where our simulations gives $\kappa = 1.0 \pm 0.1$. We have shown that this lead to the power law $w_s \propto C_a^{-\nu/(1+\nu)}$ which is close

to experimental data in [9]. Our result does not confirm the Wilkinson's argument [10] nor the proposed theory of Xu *et al.* [13]. We believe the mixing of the dynamic exponent t and the geometric exponents β and ν like in Refs. [10,13], should be done with precaution. Experience with the random resistor network at the percolation threshold [21,22], shows that different dynamic exponents may be related in an extremely complex way. Attempts to derive them by simple arguments that combine dynamic and geometric exponents, fail. This is probably due to the multi-fractal structure of the current distribution. Presumably, this is also the case here, and for that reason the mixing of dynamic and geometric exponents fails to describe our simulation results.

The authors thank E. G. Flekkøy for valuable comments. The work is supported by the Norwegian Research Council (NFR) though a “SUP” program and we acknowledge them for a grant of computer time.

- [1] K. J. Måløy, J. Feder, and T. Jøssang, *Phys. Rev. Lett.* **55**, 26881 (1985).
- [2] J.-D. Chen and D. Wilkinson, *Phys. Rev. Lett.* **55**, 1892 (1985).
- [3] R. Lenormand, E. Touboul, and C. Zarcone, *J. Fluid Mech.* **189**, 165 (1988).
- [4] M. Cieplak and M. O. Robbins, *Phys. Rev. Lett.* **60**, 2042 (1988).
- [5] P. G. de Gennes and E. Guyon, *J. Mec.* **17**, 403 (1978).
- [6] R. Chandler, J. Koplik, K. Lerman, and J. F. Willemsen, *J. Fluid Mech.* **119**, 249 (1982).
- [7] D. Wilkinson and J. F. Willemsen, *J. Phys. A* **16**, 3365 (1983).
- [8] R. Lenormand and C. Zarcone, *Phys. Rev. Lett.* **54**, 2226 (1985).
- [9] O. I. Frette, K. J. Måløy, J. Schmittbuhl, and A. Hansen, *Phys. Rev. E* **55**, 2969 (1997).
- [10] D. Wilkinson, *Phys. Rev. A* **34**, 1380 (1986).
- [11] A. Birovljev, L. Furuberg, J. Feder, T. Jøssang, K. J. Måløy, and A. Aharony, *Phys. Rev. Lett.* **67**, 584 (1991).
- [12] J.-F. Gouyet, B. Sapoval, and M. Rosso, *Phys. Rev. B* **37**, 1832 (1988).
- [13] B. Xu, Y. C. Yortsos, and D. Salin, *Phys. Rev. E* **57**, 739 (1998).
- [14] E. Aker, K. J. Måløy, A. Hansen, and G. G. Batrouni, *Transp. Porous Media* **32**, 163 (1998).
- [15] W. B. Haines, *J. Agr. Sci.* **20**, 97 (1930).
- [16] K. J. Måløy, L. Furuberg, and J. Feder, *Phys. Rev. E* **53**, 966 (1996).
- [17] E. W. Washburn, *Phys. Rev.* **17**, 273 (1921).
- [18] G. G. Batrouni and A. Hansen, *J. Stat. Phys.* **52**, 747 (1988).
- [19] E. Aker, K. J. Måløy, A. Hansen, and G. G. Batrouni, *Phys. Rev. E* **58**, 2217 (1998).
- [20] D. Stauffer and A. Aharony, *Introduction to percolation theory*

theory. Taylor & Francis, London, Great Britain, 1992.

- [21] L. de Arcangelis, S. Redner, and A. Coniglio, *Phys. Rev. B* **31**, 4725 (1985).
- [22] R. Rammal, C. Tannous, P. Breton, and A.-M. Tremblay, *Phys. Rev. Lett.* **54**, 1718 (1985).